Analysis of Raman lasing in integrated small-volume silicon-on-insulator racetrack resonators

M. Waldow, M. Först, and H. Kurz

Institut für Halbleitertechnik, RWTH Aachen, Germany
waldow@iht.rwth-aachen.de

Abstract. *We present a detailed simulation-based analysis of Raman lasing in small-volume silicon-on-insulator racetrack resonators. Continuous-wave Raman lasing in submicron-sized resonant waveguide devices can be expected without the need of additional electronic structures, with a significant improvement in threshold power, device footprint and laser efficiency compared to state of the art integrated Raman lasers on silicon.*

Introduction

One elementary building block within the emerging field of Silicon Photonics is an efficient integrated laser source. In the last years rapid progress in the development of Raman lasers as integrated laser sources has been made [1], [2]. So far, experimentally demonstrated silicon-based Raman lasers comprise low-loss waveguides with large cross-sections above 1.5 μm² and exhibit overall footprints larger than 5.5 mm² [1], [2]. As the stimulated Raman scattering cross section is proportional to the intensity of the pump laser inside the silicon waveguide, it is desirable to use small-size waveguides. Another benefit of small size waveguides is the strongly reduced carrier lifetime compared to large size waveguides [3], as the free carrier lifetime determines the dominating loss mechanism of free carrier absorption in Raman lasers.
By the use of racetrack resonators high quality factors over a large wavelength range can be achieved [4]. These properties make these devices well suited for integrated Raman laser cavities. In the following we will present a model for analyzing the Raman laser characteristics in integrated racetrack resonators on silicon. With this model we analyze for the first time Raman lasing in ultrasmall waveguide resonators on silicon. We show that it is possible to develop a Raman laser with submicron-sized waveguides based on a racetrack resonator with a magnificent improvement in threshold power, laser efficiency, device footprint and without the need of additional electronic structures.

Modeling

Figure 1 shows a schematic view of the racetrack resonator structure studied here. The resonator is pumped with laser light at the pump wavelength λ_p, which is coupled to the resonator and generates the laser signal at the Stokes wavelength λ_s by stimulated Raman scattering. The amount of power coupled to or from the resonator is described by power coupling coefficients κ_p^2 and κ_s^2 at the pump and Stokes wavelengths.
The propagation of pump and Stokes powers (P_p, P_s) per resonator roundtrip can be described by two coupled differential equations [5], [6]. Within our model pump depletion, two photon absorption (TPA) and free carrier absorption (FCA) are included. Here, $\alpha_{p/s}$ are the linear waveguide losses at the pump and Stokes wavelengths, g_R is the Raman gain coefficient and β=0.5 cm/GW is the TPA coefficient of silicon [1], [2].

$$\frac{dP_p}{d\xi} = -\alpha_p P_p - \frac{g_R}{A_{eff}}\frac{\lambda_s}{\lambda_p} P_s P_p - \frac{\beta}{A_{eff}}\left(P_p^2 + 2P_p P_s\right) - \sigma(\lambda_p) N P_p \qquad (1)$$

$$\frac{dP_s}{d\xi} = -\alpha_s P_s + \frac{g_R}{A_{eff}} P_p P_s - \frac{\beta}{A_{eff}}\left(P_s^2 + 2P_p P_s\right) - \sigma(\lambda_s) N P_s \qquad (2)$$

In the last terms of Eqs. (1) and (2), σ represents the wavelength dependent FCA cross section and N is the charge carrier density resulting from TPA.

$$N = \frac{\beta \tau_{eff}}{2E_p A_{eff}^2}\left(P_p + P_s\right)^2 \qquad (3) \qquad \sigma(\lambda) = 1.45 * 10^{-17}\left(\frac{\lambda}{1.55\mu m}\right)^2 cm^2 \qquad (4)$$

In Eq. (3) τ_{eff} is the effective carrier lifetime inside the silicon waveguide and E_p is the photon energy at the pump wavelength, where the assumption $E_p \approx E_s$ is made. For an adequate description of the nonlinear interaction area we use an overlap integral between the mode profiles at pump and Stokes wavelengths based on the definition presented in [7]:

$$A_{eff} = \frac{\mu_0}{\varepsilon_0 n_{Si}^2} \frac{\left|\iint_{Atot} \Re\{\vec{E}_p \times \vec{H}_p\}\vec{e}_z dxdy\right| * \left|\iint_{Atot} \Re\{\vec{E}_s \times \vec{H}_s\}\vec{e}_z dxdy\right|}{\iint_{ASi} \left|\vec{E}_p\right|^2 * \left|\vec{E}_s\right|^2 dxdy} \qquad (5)$$

In order to describe the resonator behavior, the boundary conditions at the coupling region of the resonator have to be included. Inside the resonator the following equations, for pump and Stokes power for the i^{th} roundtrip inside the resonator can be derived:

$$P_s''(i) = t_s^2 P_s'(i-1), \; P_p''(i) = t_p^2 P_p'(i-1) + P_p'(0) + 2t_p\kappa_p\sqrt{P_p'(0)P_p'(i-1)}, \; t_{p/s}^2 + \kappa_{p/s}^2 = 1 \qquad (6)$$

It is assumed, that pump and Stokes wavelengths match precisely a resonance wavelength of the racetrack resonator. Equations (1)-(6) are solved iteratively until a steady state for pump and Stokes power after n iterations is reached. The output power of the Raman laser at the Stokes wavelength is then calculated as $P_{Raman}=\kappa_s^2 P_s'(n)$.

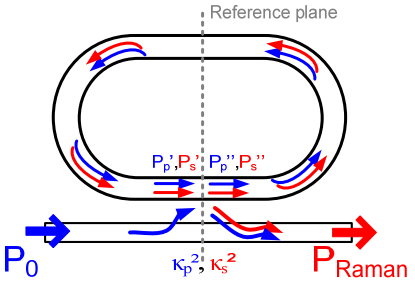

Fig.1: Schematic view of a racetrack resonator. P_0 represents the initial pump power, P_{Raman} the output power of the Raman laser at the Stokes wavelength λ_s. $\kappa_{p/s}^2$ describe the wavelength dependent coupling coefficients between bus waveguide and resonator.

Results and discussion

In order to demonstrate the reliability and performance of our model we apply the equations above to an experimentally demonstrated Raman laser based on a racetrack resonator of large-size SOI rib waveguides [2]. For all presented modeling results in this contribution a pump wavelength of λ_p=1550nm and a Stokes wavelength of λ_s=1686nm is used. All coupling coefficients for the different resonators were also taken from [2].

Used modeling parameters as given in [2] are L_{cav}=3 cm, $\alpha_{s/p}$=0.6±0.1 dB/cm, τ_{eff}=1 ns and g_R=9.5 cm/GW.

Figure 2 shows the Raman laser output power P_{Raman} for different input pump powers P_0. Solid lines represent our numerical simulations and corresponding measured data points are taken from [2]. Obviously, our modeling results are in excellent agreement with the experimental data, demonstrating the suitability of our model to analyze Raman lasing in SOI racetrack resonator structures.

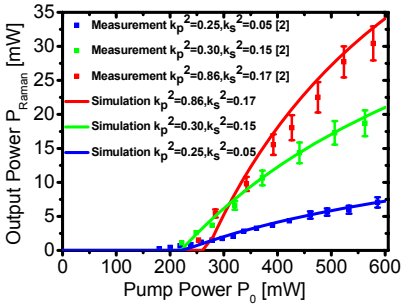

Fig.2: Output power Raman laser over input pump power. Shown are the experimental data taken from Ref. [2] and our simulation results (solid lines) for different coupling coefficients $\kappa_{p/s}^2$.

Subsequently we apply our model to resonator structures with ultrasmall cross sections. We consider SOI waveguides of 400 nm width and 340 nm height. After simulating the mode profiles for pump and Stokes wavelengths with the finite element software HFSS the effective modal area was calculated to A_{eff}=0.15 µm². For the Raman gain coefficient g_R we used the value of g_R=30 cm/GW, which has been experimentally determined for small-size waveguides with comparable cross-sections [8], [9]. We model a ring resonator of 100 µm radius equivalent to about a 24-fold reduction in resonator length compared to Raman lasers on silicon demonstrated up to now.

For this resonator configuration power coupling factors of κ_p^2=0.12 and κ_s^2=0.09 were calculated using coupled mode theory. The value of κ_p^2 is close to critical coupling at the chosen resonator geometry for state of the art waveguide losses of 2 dB/cm [4], [10]. The effective carrier lifetime is determined by interface and surface recombination velocities and can be estimated to τ_{eff}=1.2ns for the given waveguide geometry [3]. Figure 3(a) shows the Raman output power P_{Raman} versus input pump power P_0 for different linear propagation losses $\alpha=\alpha_p=\alpha_s$. The laser threshold power increases with increasing linear waveguide losses and the Raman output power saturates at higher input powers due to TPA induced FCA. An extremely low threshold power level of 6.9 mW for state of the art waveguide losses can be expected. This presents about a threefold reduction in power threshold level compared to the lowest threshold level presented so far for large size rib waveguide resonators [1].

Fig. 3(b) shows the Raman output power P_{Raman} over input pump power P_0 for different effective carrier lifetimes τ_{eff}. It becomes clear, that at shorter effective carrier lifetimes larger laser efficiencies can be reached. Assuming an effective carrier lifetime of τ_{eff}=50ps, which has already been demonstrated using a p-i-n-diode ring resonator in small size waveguides [11], a total laser efficiency of 30.1 % at P_0=100 mW can be achieved. This represents more than twice of the highest efficiency of silicon Raman lasers realized so far .in large size rib waveguides.

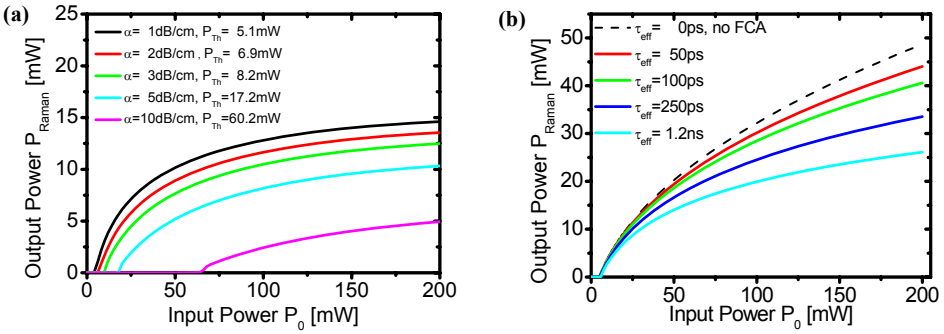

Fig. 3: (a) Raman output power P_{Raman} vs. input pump power P_0 for different linear propagation losses $\alpha=\alpha_p=\alpha_s$ and τ_{eff}=1.2 ns. (b) Raman output power P_{Raman} vs. input pump Power P_0 for different effective carrier lifetimes τ_{eff} and α=2 dB/cm.

Conclusion

An effective model to predict the output characteristics of racetrack resonator based integrated continuous wave Raman lasers on silicon is presented, predicting better performance as reported up to now. The key point is the scalability to ultrasmall SOI waveguides, with small effective core areas and low carrier lifetimes, allowing integrated Raman laser on silicon with higher efficiencies, lower threshold power levels and about a 140-fold footprint reduction compared to state of the art Raman lasers.

References

[1] H. Rong, S. Xu, Y. Kuo, V. Sih, et al., "Low-threshold continuous-wave Raman silicon laser", Nature Photonics, vol. 1, pp. 232-237, 2007.

[2] H. Rong, Y. Kuo, S. Xu, A. Liu, et al., "Monolithic integrated Raman silicon laser", Optics Express, vol. 14, pp. 6705-6712, 2006.

[3] D. Dimitropolous, R. Jhaveri, R. Claps, J. C. S. Woo, and B. Jalali, "Lifetime of photogenerated carriers in silicon-on-insulator rib waveguides", Appl. Phys. Lett., vol. 86, 2005.

[4] J. Niehusmann, A. Vörckel, P. H. Bolivar, T. Wahlbrink, W. Henschel, and H. Kurz, „Ultrahigh-quality-factor silicon-on-insulator microring resonator, Optics Express, vol. 24, pp. 2861-2863, 2004.

[5] M. Krause, H. Renner and E. Brinkmeyer, "Analysis of Raman lasing characteristics in silicon-on-insulator waveguides", Optics Express, vol. 12, pp. 5703-5710, 2004.

[6] F. De Leonardis and V. M. N. Passaro, "Modelling of Raman amplification in silicon-on-insulator optical microcavities", New Journal of Physics, vol. 9, 2007.

[7] C. Koos, L. Jacome, C. Poulton, J. Leuthold and W. Freude, "Nonlinear silicon-on-insulator waveguides for all-optical signal processing", Optics Express, vol. 15, pp. 5976-5990, 2007.A. Liu,

[8] R. L. Espinola, J. I. Dadap, R. Osgood, et al., "Raman amplification in ultrasmall silicon-on-insulator wire waveguides", Optics Express, vol. 12, pp. 3713-3718, 2004.

[9] J. I. Dadap, R. L. Espinola, R. M. Osgood, et al., "Spontaneous Raman scattering in ultrasmall silicon waveguides", Opt. Lett., vol. 29, pp. 2755-2757, 2004.

[10] S. Xiao, M. H. Khan, H. Shen , and M. Qi, "Compact silicon microring resonators with ultra-low propagation loss in the C band", Optics Express, vol. 15, pp. 14467-14475, 2007.

[11] S. F. Preble, Q. Xu, B. S. Schmidt, and M. Lipson, "Ultrafast all-optical modulation on a silicon chip", Opt. Lett., vol. 30, pp. 21, 2005.